Association of tamoxifen resistance and lipid reprogramming in breast cancer.

Susanne Hultsch[1*], Matti Kankainen[1], Lassi Paavolainen[1], Ruusu-Maaria Kovanen[1], Elina Ikonen[2], Sara Kangaspeska[1,3], Vilja Pietiäinen[1], and Olli Kallioniemi[1,4]

1. Institute for Molecular Medicine Finland, FIMM, Helsinki Institute for Life Sciences (HiLIFE), University of Helsinki, Helsinki, Finland,
2. Department of Anatomy, Faculty of Medicine, University of Helsinki, Helsinki, Finland,
3. Present affiliation: Helsinki Innovation Services (HIS)
4. Department of Oncology and Pathology, Karolinska Institutet and the Science for Life Laboratory (SciLifeLab), Stockholm, Sweden

Abstract

Tamoxifen treatment of estrogen receptor (ER)-positive breast cancer reduces mortality by 31%. However, over half of advanced ER-positive breast cancers are intrinsically resistant to tamoxifen and about 40% will acquire the resistance during the treatment. In order to explore mechanisms underlying endocrine therapy resistance in breast cancer and to identify new therapeutic opportunities, we created tamoxifen-resistant breast cancer cell lines that represent the luminal A or the luminal B. Gene expression patterns revealed by RNA-sequencing in seven tamoxifen-resistant variants were compared with their isogenic parental cells. We show that tamoxifen resistance cannot simply be explained by altered expression of individual genes, common mechanism across all resistant variants, or the appearance of new fusion genes. Instead, the resistant cell lines shared altered gene expression patterns associated with cell cycle, protein modification and metabolism, especially with the cholesterol pathway. In the tamoxifen-resistant T-47D cell variants we observed a striking increase of neutral lipids in lipid droplets as well as an accumulation of free cholesterol in the lysosomes. Tamoxifen-resistant cells were also less prone to lysosomal membrane permeabilization (LMP) and not vulnerable to compounds targeting the lipid metabolism. However, the cells were sensitive to disulfiram, LCS-1, and dasatinib. Altogether, our findings highlight a major role of LMP prevention in tamoxifen resistance, and suggest novel drug vulnerabilities associated with this phenotype.

Introduction

Approximately two thirds of breast cancers are estrogen receptor (ER) positive. As the receptor stimulates proliferation of mammary epithelial cells, it is also an important target in anti-hormonal cancer therapy. One of the most prescribed ER antagonists for first line therapy is tamoxifen (Chang 2012; Harper and Walpole 1967) that has helped millions of women since its discovery 50 years ago (Jordan 2003). However, *de novo* or acquired drug resistance towards tamoxifen is a notable problem and the later affects approximately 40% of patients receiving tamoxifen (Ring and Dowsett 2004). Resistance mechanisms involve alterations in the direct targets of tamoxifen (Karnik et al. 1994; Toy et al. 2013; D. R. Robinson et al. 2013; Giacinti et al. 2006), as well as activation of alternative signaling pathways (Gee et al. 2005) among others (Ring and Dowsett 2004; Osborne and Schiff 2011).

In addition to its intended anti-cancer effects, tamoxifen is known to have both direct and indirect effects on the cellular lipid metabolism. It has been shown to reduce blood cholesterol levels (Caleffi et al. 1988)

and to be protective against cardiovascular diseases (Rutqvist and Mattsson 1993; McDonald et al. 1995). However, approximately 43% of the patients treated with tamoxifen develop hepatic steatosis, including the accumulation of neutral lipids to lipid droplets in hepatic cells (Nishino et al. 2003). Tamoxifen can regulate the lipid balance e.g by binding to the microsomal antiestrogen binding sites (AEBS), which are associated with cholesterol metabolism (Kedjouar et al. 2004; de Medina et al. 2011). This mechanism has been linked to control cell growth, differentiation and apoptosis in the presence of reactive oxygen species (ROS) and has been established as another mode by which tamoxifen induces cytotoxicity (Payré et al. 2008; Bekele et al. 2016).

On the other hand, reprogrammed metabolism is one hallmark of cancer cells (Pavlova and Thompson 2016) and has recently been suggested as a new mode of drug resistance in cancer therapy (Montopoli et al. 2011; Bacci et al. 2016; C.-L. Chen et al. 2016). The metabolic intermediates can supply cancer cells with membrane phospholipids, with energy through the β-oxidation pathway or with pro-tumorigenic lipid-signaling molecules such as lysophosphatidic acid (Zaidi et al. 2013). Some studies even suggested a role of cholesterol metabolism in tamoxifen resistance (Pitroda et al. 2009; Tiwary et al. 2011) and Borgguist et al. showed an improved clinical outcome for ER-positive breast cancer patients receiving cholesterol-lowering medication during their adjuvant endocrine therapy (Borgquist et al. 2017).

In the present study, we have delineated mechanisms underlying tamoxifen resistance by extending our drug screening and exome sequencing analyses on tamoxifen-resistant cell lines (Kangaspeska et al. 2016) by performing RNA-sequencing on the tamoxifen-resistant and their isogenic, tamoxifen-sensitive parental cell lines, and searched for genes and pathways that may be involved in the acquired resistance. Differential gene expression and pathway analysis confirmed that endocrine resistance is not triggered by one common mechanism but involves several functional pathways, depending on the cell type (Kangaspeska et al. 2016). Through the integration with public data (McBryan et al. 2015), the usefulness of our breast cancer cell line model was assessed and the relevance of the identified transcriptomic alterations verified in this patient cohort. By focusing on the isogenic T-47D cell variants, we showed that genes in the cholesterol pathway were differentially expressed between tamoxifen-sensitive and tamoxifen-resistant cells. These results were supported by a striking accumulation of lysosomal cholesterol upon tamoxifen treatment, increased neutral lipid amounts after the development of resistance. Markedly, tamoxifen treated cells were also found to be less prone to lysosomal membrane permeabilization, suggesting that altered lysosomal integrity may confer resistance to tamoxifen. Finally, using high-content phenotypic drug sensitivity profiling of 33 drugs targeting lipid metabolism as well as inducing lysosomal membrane leakage, we identified drug candidates for overwriting the tamoxifen resistance and potentially being beneficial for breast cancer patients unresponsive to tamoxifen.

Methods

Cell culture

The development, characterization and culturing of the tamoxifen-resistant and their isogenic parental cell lines has been published previously (Kangaspeska et al. 2016). If not otherwise stated, the parental cell lines (luminal A: MCF-7, T-47D, ZR-75-1, luminal B: BT-474) were cultured without tamoxifen and the tamoxifen-resistant cell lines, marked with Tam throughout this study (MCF-7 Tam1, T-47D Tam1 & Tam2, ZR-75-1 Tam1 & Tam2, BT-474 Tam1 & Tam2) were supplemented with 1 µM 4-OH-tamoxifen (Sigma).

RNA-sequencing and data analysis of cell line data

RNA isolation, library preparation, sequencing, and data-analysis were done as explained in Kumar A et al. (Kumar et al. 2017). Briefly, total RNA was isolated using miRNeasy kit (Qiagen) and its quality was controlled by using the Agilent Bioanalyzer with the RNApico chip (Agilent). Qubit RNA-kit (Life Technologies) was used to quantitate RNA amount per sample. The strand-specific paired-end RNA-sequencing library was prepared then with ScriptSeq™ Complete kit for human/mouse/rat (Illumina). The library preparation included the ribodepletion of rRNA from 1 µm of total RNA and generation of double stranded cDNA by revers transcription with random hexamers for generation of cDNA. SPRI beads (Agencourt AMPure XP) were used to purify the libraries and to remove fragments less than 200 bp in length. The mean fragment size ranged from 300 to 400 nucleotides. The library quality was evaluated on the High Sensitivity chip by Agilent Bioanalyzer (Agilent). The paired-end sequencing was performed using the Illumina HiSeq 2000 (Illumina) instrument according to the manufacturer's instructions.

RNA-sequencing data analysis was performed as described in detail in Kumar et al. (Kumar et al. 2017) and included pre-processing of read data, gap-aware alignment of the read data to the human reference genome (Ensembl GRCh38) with the guidance of the EnsEMBL reference gene models (EnsEMBL v80), read summarization against EnsEMBL v80 gene features, and identification of fusion genes. Fusion genes were detected using FusionCatcher, which was applied to raw, un-processed read files with default parameters (Nicorici et al. 2014). The raw and processed sequencing data have been deposited in the GEO database [GEO: GSE111151].

Integration of public and cell-line transcriptomic data and differential expression analysis

Public patient transcriptome data (McBryan et al. 2015) was downloaded from GEO database (Barrett et al. 2013) and analyzed as cell line sequencing data, but using the EnsEMBL v82 gene features in all steps. Alignment files were combined with alignment files from the cell-line samples and count estimates were generated against EnsEMBL v82 gene features using subreadR (Liao, Smyth, and Shi 2014). Count data was then assigned to EnsEMBL information using biomaRt (Smedley et al. 2015), normalized using the trimmed mean of M-values (TMM) method (M. D. Robinson and Oshlack 2010), converted to CPM (counts per million) estimates using edgeR (M. D. Robinson, McCarthy, and Smyth 2010), corrected for the batch effect associated with the study origin using limma (Smyth and Speed 2003), and filtered for lowly expressed features showing log2 expression ≤ 1 in over half of samples. Default parameters were used. In the lack of biological replicates, differentially expressed genes were identified as those with a log2 ratio of >= |1| and CPM difference of >= |10| against its matched parental cell line. Further, we used Enricher (E. Y. Chen et al. 2013; Kuleshov et al. 2016) with the list of differentially expressed genes to determine pathways that were involved in the development of tamoxifen resistance for each parental vs. resistant cell line comparison. Log2 ratios of differentially expressed of the cell lines were visualized using heat maps. In the heat map analysis, genes and samples were ordered using unsupervised complete linkage clustering with Euclidean distance measure (Kangaspeska et al. 2016). Patient and cell line data was visualized using principle component analysis and heat maps as described above using biomaRt to extract cholesterol genes under the reactome.ID R-HSA-191273.

Measurement of triglycerides and cholesterol esters

Parental and resistant T-47D cells were plated on 6-well plates and grown in their default media +/- 1 µM 4-OH-tamoxifen for 72 h in triplicates. Cells were scraped in 0.2 N NaOH for lipids extraction as previously described (Bligh and Dyer 1959). Cell lysates were also examined for protein amount. Free cholesterol, cholesterol esters and triglycerides were resolved on TLC plates using hexane/diethyl ether/acetic acid (80:20:1) as the mobile phase prior to the visualization of lipids by charring. The lipid bands were

quantified by ImageJ (Schneider, Rasband, and Eliceiri 2012) from scanned plates and the lipid amounts were determined based on the standard curves for triglycerides, cholesterol esters and free cholesterol.

Immunofluorescence staining and Western blotting

Parental and resistant T-47D cells were seeded on coverslips and grown in the default media +/- tamoxifen for 72 h. Cells were fixed with 4 % paraformaldehyde for 20 minutes at room temperature, and permeabilized with 0.3 % Triton X-100 for 5 minutes, followed by 30 min blocking with 3 % BSA-PBS at 37 °C. The primary and secondary antibodies were diluted in 1 % BSA-PBS and consecutively incubated for 60 and 30 min at 37 °C. For detection of free cholesterol, cells were stained with 0.05 % filipin (Sigma) in 10% FBS–PBS blocking solution for 30 minutes at 37 °C. Antibodies were prepared in 5 % FBS-PBS and incubated as described above. Nuclei were stained with DRAQ5 (Biostatus). For detecting lipid droplets, LipidTOXGreen neutral lipid stain (ThermoFisher Scientific) was diluted 1:200 in PBS to stain freshly fixed coverslips following the manufactures protocol and detecting the nuclei with Hoechst. Stained coverslips were mounted with Prolong Gold anti-fade reagent (Invitrogen) and imaged with a Nikon 90i microscope (Nikon). For Western blotting, cells were grown on 10 cm dishes, and lysed in Laemmli buffer. Immunoblotting was performed as previously described (Leivonen et al. 2009) using the Odyssey Blocking Buffer (Licor) for blocking and the antibody dilutions. The protein intensity was quantified with ImageJ and normalized to β-actin/-tubulin, respectively. Information about the antibodies and their dilution used for immunofluorescence as well as Western blotting is available at Additional File 1.

Lysosomal membrane permeabilization (LMP) assay

In order to measure the integrity of lysosomal membranes, we performed the detection of damaged lysosomes by galectin-1 and -3 translocation according to the previously published protocol (Aits, Jäättelä, and Nylandsted 2015). We first established that galectin-3 was in our cell lines a more reliable marker to detect its translocalization to the lysosomes compared to galectin-1. We then seeded 2000 cells/well of T-47D, T-47D Tam1 and Tam2 on PE Cell-Carrier 384-well plate +/- 1 µM 4-OH-tamoxifen. After 72 h incubation, 1 mM LLMOe was added as LMP induction control and incubated for 1 h. Cells were then fixed with 4 % PFA and stained with galectin-3 detected with Alexa 568 (461nm), ceruloplasmin as cell segmentation marker detected with Alexa 488 (488 nm, Additional file1) and Hoechst (405nm) for detection of the nuclei. 16 fields-of-view were acquired with the two sCMOS cameras (2160x2160 pixels) containing Opera Phenix HCS system (PerkinElmer) in a widefield mode with the 40x water immersion objective (NA 1.1). Exposure time and laser power were kept constant for each individual staining across different cell lines and conditions. We utilized the Columbus Image Data Storage and Analysis System (PerkinElmer) to analyze the multi-channel images. First, the images were preprocessed to correct non-uniform illumination. Next, individual nuclei were segmented from the Hoechst channel. The minimum area of a nucleus was set to 30 µm² to remove the detection of debris in the image background. Starting from the detected nuclei, the segmented regions were propagated to cover cell cytoplasm stained with ceruloplasmin. The cells that touched the image border were discarded. Finally, spot detection was used to segment galectin-3 stained spots. The maximum radius of the spots was set to 1 µm. We defined cells with more than 1 spot as galectin-3 positive to exclude false positive detection. Further, we calculated the percentage of galectin-3 positive cells and the average spots per cell.

Drug sensitivity and resistance testing (DSRT) and high-content phenotypic drug profiling

33 compounds that target lipid and cholesterol metabolism, or induce LMP, were selected for the DSRT by literature and vendor research (Additional file 2). As in the previous DSRT screens (Kangaspeska et al.

2016; Pemovska et al. 2013), the dissolved drugs were transferred in five different concentrations covering a 10 000-fold concentration range into 384-well plates in duplicates mirrored after column 12. 1500 cells of T-47D parental, Tam1, and Tam2 cells were then seeded into the wells in normal growth media on columns 1-12 of each plate and in media supplemented with 1 μM 4-OH-tamoxifen on columns 13-24. The cells were then incubated for 72 h at 37 °C and cell viability was measured by CellTiter-Glo (CTG) Cell Viability Assay (Promega) with the PHERAstar plate reader. Data was normalized to negative (DMSO only) as well as positive (100 μmol/l benzethonium chloride) controls, logistic dose response curves fitted using the Marquardt-Levenberg algorithm, and Drug Sensitivity Score (DSS) calculated as described previously (Yadav et al. 2014), and implemented in the in-house bioinformatics analysis pipeline Breeze.

For the high-content phenotypic drug profiling, plates were fixed with 4 % PFA-PBS after incubation with drugs for 72 h, and stained with LipidTOXGreen neutral lipid stain (ThermoFisher Scientific) diluted 1:200 in PBS and Hoechst for nuclei detection. 25 fields-of-view per well were acquired with the PE Opera Phenix HCS system (PerkinElmer) in a confocal mode with the 40x water immersion objective (NA 1.1). Exposure time and laser power were kept constant for each individual staining across different cell lines and conditions. Images were analyzed using a custom pipeline to measure LipidTOXGreen signal and image-based DSS based on cell counts. Images were preprocessed by applying flatfield correction using CIDRE method (Smith et al. 2015), and then stitching corrected 25 fields-of-view images to a single image of a well for each channel. The stitching was done to enable the analysis of cells crossing internal borders of images. The stitching produced images of approximately 10400^2 pixels in size which were resampled to 5200^2 pixels to reduce computational capacity needed for image analysis. Images were analyzed with CellProfiler 2.2.0 (Kamentsky et al. 2011). First, nuclei were segmented from the Hoechst channel using Otsu thresholding followed by separation of touching nuclei with watershed transform on distance transformed image. LipidTOXGreen channel was segmented using adaptive Otsu thresholding and propagation outwards from individual nuclei. The LipidTOXGreen signal was measured in segmented regions for each individual cell. Logistic dose response curves were fitted to cell counts to calculate image-based DSS in Breeze.

Results

Each tamoxifen-resistant cell line develops its individual gene expression and fusion gene profile

RNA-sequencing was performed to detect differentially expressed genes and pathways between parental and resistant cell lines. Between 85 and 181 million filtered reads were obtained per sample (Additional file 3), providing means to obtain expression estimates between 33,600 and 37,000 genes per sample. We determined differential gene expression as log2 change of >|1|, and the difference of gene expression > |10| CPM between the resistant clone and its isogenic parental cell line (see Methods). Using this filtering, we identified >1200 differentially expressed genes in MCF-7- and T-47D-derived cells, and <400 genes in BT-474- and ZR-75-1-derived cells. On average 59 % of differentially expressed genes were upregulated in the majority of resistant cell lines (Table 1). Interestingly, only about 35 % of altered genes in T-47D as well as BT-474, and only 24 % in ZR-75-1 were shared between the resistant cells derived from the same parental cell line and sampled at the same time point (Additional figure 1A). Additionally, no common differentially expressed genes were identified, highlighting that each of the resistant cell lines had developed resistance through a distinct molecular pattern (Figure 1A and B). Nevertheless, common genes (*SERPINA1, PLXDC2, NAV1*, *DOCK10* and *LRP1*) with altered expression were detected in the luminal A cell lines (Additional figure 1B). No shared fusion genes across the cell lines were detected apart from the read-through fusions *ABCC11-ABCC12* and *TRIM3-HPX* (Additional file 4).

Tamoxifen-resistant cell lines resemble tamoxifen-treated patient cases

To compare the tamoxifen-resistant cell line models with breast cancer patient samples, we reanalyzed the McBryan et al. RNA-sequencing data (McBryan et al. 2015). Following the analysis with our RNA-sequencing pipeline and correction for batches (patient samples and cell lines), we determined differentially expressed genes between primary and metastatic tumors and integrated the data with the transcriptome data from our cell lines. The results were in line with McBryan's et al., and indicated that only about 2.5 % of differentially expressed genes were shared between all the patients (Figure1 C). Interestingly, we found that patient-specific expression profiles clustered together with the expression of the luminal A cells (Figure 1D). Furthermore, *SERPINA1*, which was differentially expressed in the tamoxifen-resistant luminal A cell lines (being upregulated in MCF-7 Tam1 and downregulated in T-47D Tam1, T-47D Tam2, ZR-75-1 Tam1 and ZR-75-1 Tam2), also changed its expression in the patient samples (being up-regulated in all three metastatic tumors). *CP* (Ceruloplasmin), a gene that was highly upregulated in the resistant T-47D cell lines (240-290 fold-increase) as well as MCF-7 Tam1 (26 fold-increase), was also found to be overexpressed in all the 3 metastatic patient samples ranging from 12-fold increase (patient 2) to 50-57 fold increase (patient 1 and 3, respectively Additional file 5).

Triglyceride and cholesterol ester amounts are increased in the resistant T-47D cell lines

To reveal pathways associated with tamoxifen resistance, we analyzed the differentially expressed genes with Enrichr (E. Y. Chen et al. 2013; Kuleshov et al. 2016). Based on the Reactome 2016 analysis, we observed multiple enriched pathways in different resistant cell lines (Table 2). The most striking differences were found in the T-47D Tam1 and Tam2 cells, which displayed changes in metabolism associated genes, especially those involved in cholesterol and related lipid metabolism (Table 2, Figure 2A).

In addition, we observed an upregulation of genes involved in cholesterol biosynthesis, which was also apparent in all metastatic patient samples from McBryan et al. study (Figure 2A). Therefore, we focused our studies on these pathways (Table 2). To investigate whether deregulation of genes involved in cholesterol biosynthesis could affect the cellular cholesterol balance, we stained cellular free cholesterol with filipin, a fluorescent cholesterol-binding compound. Notably, we observed increased intracellular amounts of free cholesterol in the resistant cells, displaying a cumulus cloud-like staining pattern (Figure 2B). To quantify the presence of major cellular lipid species e.g. cholesterol, cholesterol esters, and triglycerides, their amounts were further determined with thin layer chromatography. The total cellular free cholesterol remained unchanged, suggesting that only the distribution of free cholesterol was altered in the resistant cells. However, we observed an increase in neutral lipids (cholesterol esters and triglycerides) upon tamoxifen treatment. The increase in triglycerides was strikingly high (4 to 7 fold-increase) in resistant cells compared to parental cells. To visualize the changes in neutral lipid amounts as well as their intracellular distribution, we stained the cells with LipidToxGreen, a fluorescent dye binding specifically to neutral lipids. The analysis indicated that most of the neutral lipids accumulated in enlarged lipid droplets, which fill the cytoplasm (Figure 2C & D). Moreover, RNA sequencing results implicated that the expression of Peroxisome Proliferator-Activated Receptor gamma (*PPARG*) was upregulated in resistant cells. PPARG, which is normally expressed in a limited number of cells and regulates adipogenesis as well as expression of several lipid droplet proteins (de la Rosa Rodriguez and Kersten 2017), was upregulated in resistant cells. In addition, the ATP Binding Cassette Subfamily A Member 1 (*ABCA1*), which functions as a cholesterol efflux pump was downregulated (Additional file 5).

Tamoxifen-resistant cells show altered morphology of lysosomes, have altered processing of Cathepsin D, and are less susceptible to lysosomal membrane permeabilization

To localize the accumulated free cholesterol, we co-stained free cholesterol (filipin) with antibodies detecting the lysosomal-associated-membrane-proteins 1 and 2 (Lamp1 and Lamp2). Based on this analysis, we observed that most of the free cholesterol accumulated into lysosomes. We also discovered an increase in the amount and size of lysosomes as well as divergences in shape compared to their typical round form seen in the parental cell lines (Figure 3A & B). As the tamoxifen-resistant cells displayed a prominent phenotype with free cholesterol accumulation to structurally disturbed lysosomes, we studied the amounts of cathepsin D and its lysosomal maturation. Cathepsins are lysosomal proteins that help to maintain the homeostasis of cell metabolism and are involved in apoptotic signaling as well as in lysosomal membrane permeabilization. Furthermore, the expression of cathepsin D is known to be regulated by estrogen (Rochefort et al. 1987). The amount of cathepsin D was decreased in tamoxifen-resistant cells. As expected, we observed a decrease of mature cathepsin D (28 kDa) under tamoxifen treatment in parental and resistant cell lines, suggesting that tamoxifen can regulate the expression and/or processing of cathepsin D (Long and van den Berg 1996). Whilst addition of tamoxifen also caused an upregulation of the precursors of cathepsin D in the parental cell line, such an increase was not obvious in the resistant cell lines (Figure 3E), suggesting that the maturation of cathepsin D in the lysosomes may also be affected.

As lysosomal integrity, with cholesterol content of lysosomal membranes and cathepsin D among its regulators, plays an important role in the induction of cell death (Galluzzi, Bravo-San Pedro, and Kroemer 2014), we monitored the translocation of galectin-3 to detect LMP. Given that galectin-3 translocation to the lysosomes was not detected in the parental cells when grown without tamoxifen, and that only very few tamoxifen-treated cells showed galectin-3 spots (Figure 3C & D), lysosomes were most likely undamaged and functional in all cells. Further, by inducing LMP with 1 mM LLOMe we were able to observe that tamoxifen treated resistant cells were less susceptible to LMP compared to the parental cell line, having only 51-53% of cells with galectin-3 spots under tamoxifen treatment and less galectin-3 spots per cell (Figure 3C & D). This suggests that circumvention of LMP in the resistant cells leads not only to tamoxifen resistance but may also decrease their sensitivity to other drugs.

Drug testing of tamoxifen resistant cells reveals sensitivity to dasatinib, disulfiram and LCS-1

Guided by our RNA-sequencing results we selected 33 drugs, known to affect the genes or pathways involved in lysosomal alterations and lipid metabolism as well as some drugs identified in our previous screen (Additional file 2, Kangaspeska et al. 2016). As readouts for the DSRT, we applied both enzymatic cell viability measurement (CTG) as well as a phenotypic image-based analysis using LipidToxGreen to observe neutral lipids in lipid droplets together with Hoechst to detect nuclei.

The cell viability measurement revealed drugs that reduced ATP levels in tamoxifen-resistant cells similarly to the control cells, independently of their lipid accumulation phenotype (Figure 4A, Additional file 6). Dasatinib, a dual Abl/Src inhibitor was more effective in killing the tamoxifen resistant cell lines compared with the parental cells in agreement with our previous results (Kangaspeska et al. 2016). Tamoxifen-resistant cells were more sensitive to microtubule depolymerizing drugs, such as vincristine and vinorelbine, when measured by ATP amounts. Interestingly, the T-47D Tam2 cells were especially sensitive to vinorelbine induced cytotoxicity (Figure 4A, Additional file 6). The mitotic inhibitors paclitaxel and docetaxel (microtubule stabilizers) were less effective in the T-47D Tam1 cells. (Figure 4A, Additional file 6).

The most effective drug against all the T-47D clones was disulfiram, a specific inhibitor of aldehyde-dehydrogenase (ALDH1). All the clones responded to AZD8055, a dual mTOR inhibitor, although T-47D Tam1 and Tam2 showed reduced sensitivity. Atorvastatin, which inhibits HMGCoA reductase, did not affect the CTG DSS levels (Figure 4A) but was able to reduce the cell count in the parental and even more in the T-47D Tam2 cells (Figure 4B). The SOD-1 inhibitor LCS-1 was effectively killing both parental and resistant T-47D clones, and RSL-3, a ferroptosis activator due to inhibition of glutathione peroxidase 4, induced cell death in all the cell lines, with somewhat reduced response in T-47D Tam1 (Figure 4B, Additional file 6).

To see whether any of the compounds are able to revert the lipid phenotype prior to reducing the cell viability (ATP-measurement) or induction of cell death (cell count), we specifically monitored the changes in neutral lipids by measuring the mean signal of LipidToxGreen in each cell. We then calculated the mean of these single-cell measurements to quantify the average LipidToxGreen intensity per well. The measured increase in the intensity was within the 2-fold range, and we were able to confirm the trends from the biochemical screen where we observed a neutral lipid accumulation in the resistant cell lines (Figure 2C, Figure 4C). Whereas most of the drugs had minor effects on the LipidToxGreen intensity (Additional file 7), the LXR-agonist TO901317 increased the lipid phenotype most strikingly in the parental cells, with less increase particularly in T-47D Tam1 cells (Figure 4D). In addition, methyl-b-cyclodextrin, a membrane cholesterol-depleting agent, caused a lipid droplet accumulation phenotype, mostly in the parental cell line prior to cell killing in the highest concentration (Additional file7).

Discussion

In this study, we utilized RNA-sequencing and pathway analysis to understand the underlying tamoxifen resistance and identify resistance-specific drug vulnerabilities. We revealed the involvement of lipid metabolism in tamoxifen resistance as well as pointed out potential therapeutic ways to target these pathways.

Gene expression analysis on tamoxifen-resistant cells reinforced our previous finding on breast cancer cells using a variety of molecular pathways as they acquire tamoxifen resistance (Kangaspeska et al. 2016). The difference in gene expression was reflected in the scale and scope of differentially expressed genes, and in the lack of shared genes across all the cell lines. However, a few genes were concordantly differentially expressed between the luminal A subtype (Figure 1, Additional figure 1). In agreement with this finding, the only study that has performed sequential tumor transcriptome analysis on patients developing endocrine resistance, also identified less than 3% of differentially expressed genes across patients (McBryan et al. 2015). We reanalyzed the McBryan *et al.* data set and confirmed this result (Figure1 C). Despite the overall transcriptome profiles being distinct across the resistant cell lines, we were able to identify five genes that were concordantly differentially expressed in the luminal A subtype resistant cells (Additional figure 1B). Of these, *SERPINA1,* encoding for a serine protease inhibitor primarily targeting elastase, is known to bind ER in a 17β-estradiol (E2) - independent manner, which leads to an increase in its expression (Chan et al. 2015). In our resistant lines, *SERPINA1* expression increased in MCF-7 Tam1 and decreased in the resistant clones of T-47D and ZR-75-1 (Additional file 5). This could be due to the down- and upregulation of ER in these cell lines (Kangaspeska et al. 2016). Interestingly, in all three metastatic samples from the McBryan *et al.* study, we observed an increase in *SERPINA1*, which is accompanied by a slight increase of *ESR1* transcription (Additional file 5). Pathway analysis of the

differentially expressed genes identified several paths involved in acquired tamoxifen resistance (Table 2, Figure 2A).

In this study, we investigated the tamoxifen-induced changes observed in lipid metabolism (Table 2, Figure 2). In addition to detecting an increase in expression of genes linked to cholesterol biosynthesis in the resistant cell lines, we also made the equivalent finding in a patient's metastatic tissue (Figure 2A). As the metastasis was found in the liver (McBryan et al. 2015), the observed lipid metabolism pathway profiles have to be interpreted with caution. Nevertheless, our findings suggest that the lipid phenotypes could already develop in the breast cancer cells (Luo et al. 2017) and is not solely induced by the liver environment. Further, our studies with the T-47D tamoxifen-resistant cell lines show an increase of free cholesterol in lysosomes (Figure 2B, Figure 3A & B, Suárez et al. 2004). Additionally, we observed an increase in cholesterol esters (Figure 2C), suggesting that the tamoxifen-resistant cells can convert the excess cholesterol to cholesterol ester storage. We also observed a striking enlargement of the lysosomal compartment. As lysosomes and lysosomal proteins have recently been recognized to play a key role in the resistance to a wide spectrum of commonly used anticancer drugs (Hämälistö and Jäättelä 2016), our findings suggest that excess tamoxifen could be stored in these enlarged lysosomes, and its sequestration could contribute to the resistance of the cells to tamoxifen.

It has been shown that accumulation of cholesterol prevents lysosomal membrane permeabilization (Appelqvist et al. 2011), a process which leads to different forms of cell death such as apoptosis, necroptosis, necrosis and ferroptosis (Galluzzi, Bravo-San Pedro, and Kroemer 2014). However, not only cholesterol but also an increase in Lamp1 and Lamp2 as well as downregulation of cathepsins have been shown to influence the lysosomal stability (Fehrenbacher et al. 2008; Aits and Jäättelä 2013; Liaudet-Coopman et al. 2006). Indeed, our data on the resistant cells shows an increase in cholesterol, Lamp1 and Lamp2, as well as a decrease in cathepsin D (Long and van den Berg 1996, Figure 2B, Figure 3A, B and E). A short-term tamoxifen treatment diminished directly the LLOMe-induced LMP, measured by the recruitment of galectin-3 into lysosomes. The T-47D Tam1 and Tam2 were even more resistant towards LMP (Figure 3C and D), showing that tamoxifen can hinder it, and in acquired resistance, this phenomenon is even more prominent. Thus, impeded lysosomal membrane permeabilization may additionally enhance the co-resistance to other cancer drugs during acquired tamoxifen resistance.

An enormous increase in triglycerides, stored in large lipid droplets (LDs) was observed in tamoxifen-resistant cells. Free fatty acids are enzymatically converted to triacylglycerol, and then incorporated into LDs. Packaging of excess lipids into LDs could be seen as an adaptive response to fulfilling energy supply without hindering mitochondrial or cellular redox status and keeping the concentration of lipotoxic intermediates low (Aon, Bhatt, and Cortassa 2014). Accordingly, high LDs and stored cholesterol esters in tumors are considered as hallmarks of aggressive cancer (Beloribi-Djefaflia, Vasseur, and Guillaumond 2016). LD-rich cancer cells have also been shown to be more resistant to chemotherapy (Qiu et al. 2015). We found over 3-fold upregulation of stearoyl-CoA desaturase (*SCD*), encoding for a rate-limiting enzyme in the biosynthesis of monounsaturated fatty acids, in the tamoxifen-resistant T-47Ds (Additional file 5). Whether it alone is able to induce the increase in TGs, remains to be investigated. In line with this speculation, *SCD* overexpression has been observed, in different cell types as well as in tamoxifen-induced hepatocyte steatosis, to significantly increase the rate of triglyceride synthesis (Zhao et al. 2014).

We also investigated the effects of 33 compounds that were selected to influence the lysosomal integrity and act on lipid metabolism (Additional file 2). The compounds directly affecting lipid metabolism, such

as C75, Bezafibrate, T 0070907, TO901317, and Orlistat, had no or only little effect on cell viability or the lipid phenotype (Figure 4 and Additional files 6, 7).This suggests that the T-47D cells are able to compensate the drug-induced lipid imbalance with several mechanisms. We observed that AZD8055, a drug that has been shown to reduce cellular *de novo* lipid synthesis in breast cancer cells (Qian et al. 2016) was less effective in the tamoxifen-resistant cells than in parental cells (Additional file 6), which could indicate that *de novo* lipid synthesis might not solely be responsible for the neutral lipid accumulation. Surprisingly, methyl-b-cyclodextrin caused an increase in neutral lipid accumulation prior to the cell death mainly in the parental T-47Ds as well as to a minor extant in the resistant cell lines (Additional file7). Methyl-b-cyclodextrin has been shown to sensitize cells towards tamoxifen-mediated cell death (Tiwary et al. 2011; Mohammad et al. 2014).

Disulfiram, which targets ALDH1 to increase oxidative stress, was highly effective in both parental and tamoxifen-resistant T-47D cell clones (Figure 4 and Additional file 6). The effectiveness of disulfiram is currently investigated in metastatic breast cancer in a phase II clinical trial (ClinicalTrials.gov, NCT03323346). *ALDH2*, another target of disulfiram, is upregulated in T-47D Tam1 but not in Tam2 (Additional file 5). High levels of ALDH1 have been shown to predict resistance in women treated with tamoxifen (Simões et al. 2015), but as *ALDH1A1* is expressed at very low levels in the T-47D cell lines (Additional file 5), we assume that the sensitivity to disulfiram could be due to its capability to disable antioxidation mechanisms of the cells (Hangauer et al. 2017). Further, as the effects of disulfiram are usually boosted by copper, and we additionally saw an increase in expression of the copper-binding enzyme ceruloplasmin, one would assume that disulfiram would be more effective in the tamoxifen-resistant cell lines.

Reducing the reactive oxygen species (ROS) is another mechanism by which cells avoid lysosomal induced cell death (Aits and Jäättelä 2013). We speculate that resistant T-47D cells are able to reduce oxidative stress by upregulation of *SOD1* (Additional file 5) and may therefore be less sensitive to lysosomal cell death. This hypothesis is further supported by the fact that the resistant cells were highly sensitive to the SOD1 inhibitor LCS-1. The capability of erastin to activate ferroptosis is instead inhibited by antioxidants, and it was more effective in parental than in resistant cells. The ferroptosis activator RSL-3, which inhibits the glutathione peroxidase 4, an enzyme that protects from oxygen damage, induced cell death in all the cell lines (Figure 4 and Additional file 6). This further supports the assumption that the T-47D cells are able to reduce oxidative stress and are therefore less sensitive to lysosomal cell death.

Taken together, our results highlight that tamoxifen resistant cell lines can potentially be used as a representative model for studies of tamoxifen-resistant patients. We propose that the breast cancer cells can acquire tamoxifen resistance by dysregulation of different cellular pathways, dependent on their individual molecular phenotypes. Here, we highlight the inhibition of lysosomal membrane permeabilization as one of the mechanisms to avoid cell death, whereas an increase in neutral lipids may enable the further survival of these cells. We further propose that drugs targeting cellular antioxidation machinery may be able to overcome tamoxifen resistance. Given the vulnerability of tamoxifen resistant cells to approved drugs such as disulfiram and dasatinib, it would be interesting to investigate whether these compounds could also be effective in clinical trials in tamoxifen-resistant breast cancer patients.

Acknowledgments

We acknowledge Prof. Marja Jäättelä (Danish Cancer Society Research Institute, Denmark) for comments to lysosomal membrane permeabilization assays. Anna Uro from the Ikonen laboratory (University of Helsinki) is acknowledged for technical assistance in biochemical lipid determination. High Throughput Biomedicine (HTB) unit (Laura Turunen, Maria Nurmi and Swapnil Podar), Sequencing unit (Pirkko Mattila), and High Content image Analysis (HCA) unit at the Institute for Molecular Medicine Finland (FIMM), HiLIFE, University of Helsinki, and Biocenter Finland are acknowledged of the high throughput drug profiling and high content imaging expertise. Piia Mikkonen is acknowledged for technical help with the drug screens. Sigrid Juselius Foundation, TEKES FiDiPro Fellow Grant 40294/1, Academy of Finland Centers of Excellence in Translational Cancer Biology and in Biomembrane Research, Biocentrum Helsinki grants are acknowledged for the financial contributions to this study.

References

Aits, Sonja, and Marja Jäättelä. 2013. "Lysosomal Cell Death at a Glance." *Journal of Cell Science* 126 (Pt 9): 1905–12. https://doi.org/10.1242/jcs.091181.

Aits, Sonja, Marja Jäättelä, and Jesper Nylandsted. 2015. "Methods for the Quantification of Lysosomal Membrane Permeabilization: A Hallmark of Lysosomal Cell Death." *Methods in Cell Biology* 126: 261–85. https://doi.org/10.1016/bs.mcb.2014.10.032.

Aon, Miguel A., Niraj Bhatt, and Sonia C. Cortassa. 2014. "Mitochondrial and Cellular Mechanisms for Managing Lipid Excess." *Frontiers in Physiology* 5: 282. https://doi.org/10.3389/fphys.2014.00282.

Appelqvist, Hanna, Cathrine Nilsson, Brett Garner, Andrew J. Brown, Katarina Kågedal, and Karin Ollinger. 2011. "Attenuation of the Lysosomal Death Pathway by Lysosomal Cholesterol Accumulation." *The American Journal of Pathology* 178 (2): 629–39. https://doi.org/10.1016/j.ajpath.2010.10.030.

Bacci, Marina, Elisa Giannoni, Antony Fearns, Ricardo Ribas, Qiong Gao, Maria Letizia Taddei, Gianfranco Pintus, et al. 2016. "MiR-155 Drives Metabolic Reprogramming of ER+ Breast Cancer Cells Following Long-Term Estrogen Deprivation and Predicts Clinical Response to Aromatase Inhibitors." *Cancer Research* 76 (6): 1615–26. https://doi.org/10.1158/0008-5472.CAN-15-2038.

Barrett, Tanya, Stephen E. Wilhite, Pierre Ledoux, Carlos Evangelista, Irene F. Kim, Maxim Tomashevsky, Kimberly A. Marshall, et al. 2013. "NCBI GEO: Archive for Functional Genomics Data Sets--Update." *Nucleic Acids Research* 41 (Database issue): D991-995. https://doi.org/10.1093/nar/gks1193.

Bekele, Raie T., Ganesh Venkatraman, Rong-Zong Liu, Xiaoyun Tang, Si Mi, Matthew G. K. Benesch, John R. Mackey, et al. 2016. "Oxidative Stress Contributes to the Tamoxifen-Induced Killing of Breast Cancer Cells: Implications for Tamoxifen Therapy and Resistance." *Scientific Reports* 6 (February). https://doi.org/10.1038/srep21164.

Beloribi-Djefaflia, S., S. Vasseur, and F. Guillaumond. 2016. "Lipid Metabolic Reprogramming in Cancer Cells." *Oncogenesis* 5 (January): e189. https://doi.org/10.1038/oncsis.2015.49.

Bligh, E. G., and W. J. Dyer. 1959. "A Rapid Method of Total Lipid Extraction and Purification." *Canadian Journal of Biochemistry and Physiology* 37 (8): 911–17. https://doi.org/10.1139/o59-099.

Borgquist, Signe, Anita Giobbie-Hurder, Thomas P. Ahern, Judy E. Garber, Marco Colleoni, István Láng, Marc Debled, et al. 2017. "Cholesterol, Cholesterol-Lowering Medication Use, and Breast Cancer Outcome in the BIG 1-98 Study." *Journal of Clinical Oncology: Official Journal of the American Society of Clinical Oncology* 35 (11): 1179–88. https://doi.org/10.1200/JCO.2016.70.3116.

Caleffi, M., I. S. Fentiman, G. M. Clark, D. Y. Wang, J. Needham, K. Clark, A. La Ville, and B. Lewis. 1988. "Effect of Tamoxifen on Oestrogen Binding, Lipid and Lipoprotein Concentrations and Blood Clotting Parameters in Premenopausal Women with Breast Pain." *The Journal of Endocrinology* 119 (2): 335–39.

Chan, Hei Jason, Haiqing Li, Zheng Liu, Yate-Ching Yuan, Joanne Mortimer, and Shiuan Chen. 2015. "SERPINA1 Is a Direct Estrogen Receptor Target Gene and a Predictor of Survival in Breast Cancer Patients." *Oncotarget* 6 (28): 25815–27. https://doi.org/10.18632/oncotarget.4441.

Chang, Minsun. 2012. "Tamoxifen Resistance in Breast Cancer." *Biomolecules & Therapeutics* 20 (3): 256–67. https://doi.org/10.4062/biomolther.2012.20.3.256.

Chen, Chia-Lin, Dinesh Babu Uthaya Kumar, Vasu Punj, Jun Xu, Linda Sher, Stanley M. Tahara, Sonja Hess, and Keigo Machida. 2016. "NANOG Metabolically Reprograms Tumor-Initiating Stem-like Cells through Tumorigenic Changes in Oxidative Phosphorylation and Fatty Acid Metabolism." *Cell Metabolism* 23 (1): 206–19. https://doi.org/10.1016/j.cmet.2015.12.004.

Chen, Edward Y., Christopher M. Tan, Yan Kou, Qiaonan Duan, Zichen Wang, Gabriela Vaz Meirelles, Neil R. Clark, and Avi Ma'ayan. 2013. "Enrichr: Interactive and Collaborative HTML5 Gene List Enrichment Analysis Tool." *BMC Bioinformatics* 14 (April): 128. https://doi.org/10.1186/1471-2105-14-128.

Chen, Ting, Changyuan Wang, Qi Liu, Qiang Meng, Huijun Sun, Xiaokui Huo, Pengyuan Sun, et al. 2015. "Dasatinib Reverses the Multidrug Resistance of Breast Cancer MCF-7 Cells to Doxorubicin by Downregulating P-Gp Expression via Inhibiting the Activation of ERK Signaling Pathway." *Cancer Biology & Therapy* 16 (1): 106–14. https://doi.org/10.4161/15384047.2014.987062.

ClinicalTrials.gov, NCT03323346. n.d. "Phase II Trial of Disulfiram With Copper in Metastatic Breast Cancer - ClinicalTrials.Gov." Accessed February 14, 2018. https://clinicaltrials.gov/ct2/show/NCT03323346.

Fehrenbacher, Nicole, Lone Bastholm, Thomas Kirkegaard-Sørensen, Bo Rafn, Trine Bøttzauw, Christina Nielsen, Ekkehard Weber, Senji Shirasawa, Tuula Kallunki, and Marja Jäättelä. 2008. "Sensitization to the Lysosomal Cell Death Pathway by Oncogene-Induced down-Regulation of Lysosome-Associated Membrane Proteins 1 and 2." *Cancer Research* 68 (16): 6623–33. https://doi.org/10.1158/0008-5472.CAN-08-0463.

Galluzzi, Lorenzo, José Manuel Bravo-San Pedro, and Guido Kroemer. 2014. "Organelle-Specific Initiation of Cell Death." *Nature Cell Biology* 16 (8): 728–36. https://doi.org/10.1038/ncb3005.

Gee, J. M., J. F. Robertson, E. Gutteridge, I. O. Ellis, S. E. Pinder, M. Rubini, and R. I. Nicholson. 2005. "Epidermal Growth Factor Receptor/HER2/Insulin-like Growth Factor Receptor Signalling and Oestrogen Receptor Activity in Clinical Breast Cancer." *Endocrine-Related Cancer* 12 Suppl 1 (July): S99–111. https://doi.org/10.1677/erc.1.01005.

Giacinti, Laura, Pier Paolo Claudio, Massimo Lopez, and Antonio Giordano. 2006. "Epigenetic Information and Estrogen Receptor Alpha Expression in Breast Cancer." *The Oncologist* 11 (1): 1–8. https://doi.org/10.1634/theoncologist.11-1-1.

Hämälistö, Saara, and Marja Jäättelä. 2016. "Lysosomes in Cancer-Living on the Edge (of the Cell)." *Current Opinion in Cell Biology* 39 (April): 69–76. https://doi.org/10.1016/j.ceb.2016.02.009.

Hangauer, Matthew J., Vasanthi S. Viswanathan, Matthew J. Ryan, Dhruv Bole, John K. Eaton, Alexandre Matov, Jacqueline Galeas, et al. 2017. "Drug-Tolerant Persister Cancer Cells Are Vulnerable to GPX4 Inhibition." *Nature* 551 (7679): 247–50. https://doi.org/10.1038/nature24297.

Harper, M. J., and A. L. Walpole. 1967. "A New Derivative of Triphenylethylene: Effect on Implantation and Mode of Action in Rats." *Journal of Reproduction and Fertility* 13 (1): 101–19.

Iizuka, Katsumi, Hiroyuki Niwa, Takehiro Kato, and Jun Takeda. 2016. "Dasatinib Improves Insulin Sensitivity and Affects Lipid Metabolism in a Patient with Chronic Myeloid Leukaemia." *BMJ Case Reports* 2016 (February). https://doi.org/10.1136/bcr-2015-214284.

Jordan, V. C. 2003. "Tamoxifen: A Most Unlikely Pioneering Medicine." *Nature Reviews. Drug Discovery* 2 (3): 205–13. https://doi.org/10.1038/nrd1031.

Kamentsky, Lee, Thouis R. Jones, Adam Fraser, Mark-Anthony Bray, David J. Logan, Katherine L. Madden, Vebjorn Ljosa, Curtis Rueden, Kevin W. Eliceiri, and Anne E. Carpenter. 2011. "Improved Structure, Function and Compatibility for CellProfiler: Modular High-Throughput Image Analysis Software." *Bioinformatics (Oxford, England)* 27 (8): 1179–80. https://doi.org/10.1093/bioinformatics/btr095.

Kangaspeska, Sara, Susanne Hultsch, Alok Jaiswal, Henrik Edgren, John-Patrick Mpindi, Samuli Eldfors, Oscar Brück, Tero Aittokallio, and Olli Kallioniemi. 2016. "Systematic Drug Screening Reveals Specific Vulnerabilities and Co-Resistance Patterns in Endocrine-Resistant Breast Cancer." *BMC Cancer* 16: 378. https://doi.org/10.1186/s12885-016-2452-5.

Karnik, P. S., S. Kulkarni, X. P. Liu, G. T. Budd, and R. M. Bukowski. 1994. "Estrogen Receptor Mutations in Tamoxifen-Resistant Breast Cancer." *Cancer Research* 54 (2): 349–53.

Kedjouar, Blandine, Philippe de Médina, Mustapha Oulad-Abdelghani, Bruno Payré, Sandrine Silvente-Poirot, Gilles Favre, Jean-Charles Faye, and Marc Poirot. 2004. "Molecular Characterization of the Microsomal Tamoxifen Binding Site." *The Journal of Biological Chemistry* 279 (32): 34048–61. https://doi.org/10.1074/jbc.M405230200.

Kuleshov, Maxim V., Matthew R. Jones, Andrew D. Rouillard, Nicolas F. Fernandez, Qiaonan Duan, Zichen Wang, Simon Koplev, et al. 2016. "Enrichr: A Comprehensive Gene Set Enrichment Analysis Web Server 2016 Update." *Nucleic Acids Research* 44 (W1): W90-97. https://doi.org/10.1093/nar/gkw377.

Kumar, Ashwini, Matti Kankainen, Alun Parsons, Olli Kallioniemi, Pirkko Mattila, and Caroline A. Heckman. 2017. "The Impact of RNA Sequence Library Construction Protocols on Transcriptomic Profiling of Leukemia." *BMC Genomics* 18 (1): 629. https://doi.org/10.1186/s12864-017-4039-1.

Leivonen, S.-K., R. Mäkelä, P. Ostling, P. Kohonen, S. Haapa-Paananen, K. Kleivi, E. Enerly, et al. 2009. "Protein Lysate Microarray Analysis to Identify MicroRNAs Regulating Estrogen Receptor Signaling in Breast Cancer Cell Lines." *Oncogene* 28 (44): 3926–36. https://doi.org/10.1038/onc.2009.241.

Liao, Yang, Gordon K. Smyth, and Wei Shi. 2014. "FeatureCounts: An Efficient General Purpose Program for Assigning Sequence Reads to Genomic Features." *Bioinformatics (Oxford, England)* 30 (7): 923–30. https://doi.org/10.1093/bioinformatics/btt656.

Liaudet-Coopman, Emmanuelle, Mélanie Beaujouin, Danielle Derocq, Marcel Garcia, Murielle Glondu-Lassis, Valérie Laurent-Matha, Christine Prébois, Henri Rochefort, and Françoise Vignon. 2006. "Cathepsin D: Newly Discovered Functions of a Long-Standing Aspartic Protease in Cancer and Apoptosis." *Cancer Letters* 237 (2): 167–79. https://doi.org/10.1016/j.canlet.2005.06.007.

Long, B. J., and H. W. van den Berg. 1996. "Reduced Levels of Cathepsin D Associated with Tamoxifen Resistance and Estrogen Independence in the ZR-75-1 Human Breast Cancer Cell Line." *Cancer Letters* 99 (2): 233–38.

Luo, Xiangjian, Can Cheng, Zheqiong Tan, Namei Li, Min Tang, Lifang Yang, and Ya Cao. 2017. "Emerging Roles of Lipid Metabolism in Cancer Metastasis." *Molecular Cancer* 16 (1): 76. https://doi.org/10.1186/s12943-017-0646-3.

McBryan, Jean, Ailís Fagan, Damian McCartan, Fiona T. Bane, Damir Varešlija, Sinéad Cocchiglia, Christopher Byrne, et al. 2015. "Transcriptomic Profiling of Sequential Tumors from Breast Cancer Patients Provides a Global View of Metastatic Expression Changes Following Endocrine

Therapy." *Clinical Cancer Research: An Official Journal of the American Association for Cancer Research* 21 (23): 5371–79. https://doi.org/10.1158/1078-0432.CCR-14-2155.

McDonald, C. C., F. E. Alexander, B. W. Whyte, A. P. Forrest, and H. J. Stewart. 1995. "Cardiac and Vascular Morbidity in Women Receiving Adjuvant Tamoxifen for Breast Cancer in a Randomised Trial. The Scottish Cancer Trials Breast Group." *BMJ (Clinical Research Ed.)* 311 (7011): 977–80.

Medina, Philippe de, Michael R. Paillasse, Gregory Ségala, Farid Khallouki, Severine Brillouet, Florence Dalenc, Frederic Courbon, Michel Record, Marc Poirot, and Sandrine Silvente-Poirot. 2011. "Importance of Cholesterol and Oxysterols Metabolism in the Pharmacology of Tamoxifen and Other AEBS Ligands." *Chemistry and Physics of Lipids* 164 (6): 432–37. https://doi.org/10.1016/j.chemphyslip.2011.05.005.

Mohammad, Naoshad, Parmanand Malvi, Avtar Singh Meena, Shivendra Vikram Singh, Balkrishna Chaube, Garikapati Vannuruswamy, Mahesh J. Kulkarni, and Manoj Kumar Bhat. 2014. "Cholesterol Depletion by Methyl-β-Cyclodextrin Augments Tamoxifen Induced Cell Death by Enhancing Its Uptake in Melanoma." *Molecular Cancer* 13 (September): 204. https://doi.org/10.1186/1476-4598-13-204.

Montopoli, M., M. Bellanda, F. Lonardoni, E. Ragazzi, P. Dorigo, G. Froldi, S. Mammi, and L. Caparrotta. 2011. "'Metabolic Reprogramming' in Ovarian Cancer Cells Resistant to Cisplatin." *Current Cancer Drug Targets* 11 (2): 226–35.

Nicorici, Daniel, Mihaela Satalan, Henrik Edgren, Sara Kangaspeska, Astrid Murumagi, Olli Kallioniemi, Sami Virtanen, and Olavi Kilkku. 2014. "FusionCatcher - a Tool for Finding Somatic Fusion Genes in Paired-End RNA-Sequencing Data." *BioRxiv*, November, 011650. https://doi.org/10.1101/011650.

Nishino, Mizuki, Katsumi Hayakawa, Yoshiaki Nakamura, Taisuke Morimoto, and Sumio Mukaihara. 2003. "Effects of Tamoxifen on Hepatic Fat Content and the Development of Hepatic Steatosis in Patients with Breast Cancer: High Frequency of Involvement and Rapid Reversal after Completion of Tamoxifen Therapy." *AJR. American Journal of Roentgenology* 180 (1): 129–34. https://doi.org/10.2214/ajr.180.1.1800129.

Ogrodnik, Mikolaj, Satomi Miwa, Tamar Tchkonia, Dina Tiniakos, Caroline L. Wilson, Albert Lahat, Christoper P. Day, et al. 2017. "Cellular Senescence Drives Age-Dependent Hepatic Steatosis." *Nature Communications* 8 (June): 15691. https://doi.org/10.1038/ncomms15691.

Osborne, C. Kent, and Rachel Schiff. 2011. "Mechanisms of Endocrine Resistance in Breast Cancer." *Annual Review of Medicine* 62: 233–47. https://doi.org/10.1146/annurev-med-070909-182917.

Pavlova, Natalya N., and Craig B. Thompson. 2016. "The Emerging Hallmarks of Cancer Metabolism." *Cell Metabolism* 23 (1): 27–47. https://doi.org/10.1016/j.cmet.2015.12.006.

Payré, Bruno, Philippe de Medina, Nadia Boubekeur, Loubna Mhamdi, Justine Bertrand-Michel, François Tercé, Isabelle Fourquaux, et al. 2008. "Microsomal Antiestrogen-Binding Site Ligands Induce Growth Control and Differentiation of Human Breast Cancer Cells through the Modulation of Cholesterol Metabolism." *Molecular Cancer Therapeutics* 7 (12): 3707–18. https://doi.org/10.1158/1535-7163.MCT-08-0507.

Pemovska, Tea, Mika Kontro, Bhagwan Yadav, Henrik Edgren, Samuli Eldfors, Agnieszka Szwajda, Henrikki Almusa, et al. 2013. "Individualized Systems Medicine Strategy to Tailor Treatments for Patients with Chemorefractory Acute Myeloid Leukemia." *Cancer Discovery* 3 (12): 1416–29. https://doi.org/10.1158/2159-8290.CD-13-0350.

Pitroda, Sean P., Nikolai N. Khodarev, Michael A. Beckett, Donald W. Kufe, and Ralph R. Weichselbaum. 2009. "MUC1-Induced Alterations in a Lipid Metabolic Gene Network Predict Response of Human Breast Cancers to Tamoxifen Treatment." *Proceedings of the National Academy of*

Sciences of the United States of America 106 (14): 5837–41. https://doi.org/10.1073/pnas.0812029106.

Qian, Jianchang, Yaqing Chen, Tao Meng, Lanping Ma, Lanfang Meng, Xin Wang, Ting Yu, Arie Zask, Jingkang Shen, and Ker Yu. 2016. "Molecular Regulation of Apoptotic Machinery and Lipid Metabolism by MTORC1/MTORC2 Dual Inhibitors in Preclinical Models of HER2+/PIK3CAmut Breast Cancer." *Oncotarget* 7 (41): 67071–86. https://doi.org/10.18632/oncotarget.11490.

Qiu, Bo, Daniel Ackerman, Danielle J. Sanchez, Bo Li, Joshua D. Ochocki, Alison Grazioli, Ekaterina Bobrovnikova-Marjon, J. Alan Diehl, Brian Keith, and M. Celeste Simon. 2015. "HIF2α-Dependent Lipid Storage Promotes Endoplasmic Reticulum Homeostasis in Clear-Cell Renal Cell Carcinoma." *Cancer Discovery* 5 (6): 652–67. https://doi.org/10.1158/2159-8290.CD-14-1507.

Ring, Alistair, and Mitch Dowsett. 2004. "Mechanisms of Tamoxifen Resistance." *Endocrine-Related Cancer* 11 (4): 643–58. https://doi.org/10.1677/erc.1.00776.

Robinson, Dan R., Yi-Mi Wu, Pankaj Vats, Fengyun Su, Robert J. Lonigro, Xuhong Cao, Shanker Kalyana-Sundaram, et al. 2013. "Activating ESR1 Mutations in Hormone-Resistant Metastatic Breast Cancer." *Nature Genetics* 45 (12): 1446–51. https://doi.org/10.1038/ng.2823.

Robinson, Mark D., Davis J. McCarthy, and Gordon K. Smyth. 2010. "EdgeR: A Bioconductor Package for Differential Expression Analysis of Digital Gene Expression Data." *Bioinformatics (Oxford, England)* 26 (1): 139–40. https://doi.org/10.1093/bioinformatics/btp616.

Robinson, Mark D., and Alicia Oshlack. 2010. "A Scaling Normalization Method for Differential Expression Analysis of RNA-Seq Data." *Genome Biology* 11 (3): R25. https://doi.org/10.1186/gb-2010-11-3-r25.

Rochefort, H., F. Capony, P. Augereau, V. Cavailles, M. Garcia, M. Morisset, G. Freiss, T. Maudelonde, and F. Vignon. 1987. "The Estrogen-Regulated 52K-Cathepsin-D in Breast Cancer: From Biology to Clinical Applications." *International Journal of Radiation Applications and Instrumentation. Part B, Nuclear Medicine and Biology* 14 (4): 377–84.

Rosa Rodriguez, Montserrat A. de la, and Sander Kersten. 2017. "Regulation of Lipid Droplet-Associated Proteins by Peroxisome Proliferator-Activated Receptors." *Biochimica Et Biophysica Acta* 1862 (10 Pt B): 1212–20. https://doi.org/10.1016/j.bbalip.2017.07.007.

Rutqvist, L. E., and A. Mattsson. 1993. "Cardiac and Thromboembolic Morbidity among Postmenopausal Women with Early-Stage Breast Cancer in a Randomized Trial of Adjuvant Tamoxifen. The Stockholm Breast Cancer Study Group." *Journal of the National Cancer Institute* 85 (17): 1398–1406.

Saha, Supriya K., John D. Gordan, Benjamin P. Kleinstiver, Phuong Vu, Mortada S. Najem, Jia-Chi Yeo, Lei Shi, et al. 2016. "Isocitrate Dehydrogenase Mutations Confer Dasatinib Hypersensitivity and SRC Dependence in Intrahepatic Cholangiocarcinoma." *Cancer Discovery* 6 (7): 727–39. https://doi.org/10.1158/2159-8290.CD-15-1442.

Schneider, Caroline A., Wayne S. Rasband, and Kevin W. Eliceiri. 2012. "NIH Image to ImageJ: 25 Years of Image Analysis." *Nature Methods* 9 (7): 671–75.

Simões, Bruno M., Ciara S. O'Brien, Rachel Eyre, Andreia Silva, Ling Yu, Aida Sarmiento-Castro, Denis G. Alférez, et al. 2015. "Anti-Estrogen Resistance in Human Breast Tumors Is Driven by JAG1-NOTCH4-Dependent Cancer Stem Cell Activity." *Cell Reports* 12 (12): 1968–77. https://doi.org/10.1016/j.celrep.2015.08.050.

Smedley, Damian, Syed Haider, Steffen Durinck, Luca Pandini, Paolo Provero, James Allen, Olivier Arnaiz, et al. 2015. "The BioMart Community Portal: An Innovative Alternative to Large, Centralized Data Repositories." *Nucleic Acids Research* 43 (W1): W589-598. https://doi.org/10.1093/nar/gkv350.

Smith, Kevin, Yunpeng Li, Filippo Piccinini, Gabor Csucs, Csaba Balazs, Alessandro Bevilacqua, and Peter Horvath. 2015. "CIDRE: An Illumination-Correction Method for Optical Microscopy." *Nature Methods* 12 (5): 404–6. https://doi.org/10.1038/nmeth.3323.

Smyth, Gordon K., and Terry Speed. 2003. "Normalization of CDNA Microarray Data." *Methods (San Diego, Calif.)* 31 (4): 265–73.

Suárez, Yajaira, Carlos Fernández, Diego Gómez-Coronado, Antonio J. Ferruelo, Alberto Dávalos, Javier Martínez-Botas, and Miguel A. Lasunción. 2004. "Synergistic Upregulation of Low-Density Lipoprotein Receptor Activity by Tamoxifen and Lovastatin." *Cardiovascular Research* 64 (2): 346–55. https://doi.org/10.1016/j.cardiores.2004.06.024.

Tiwary, Richa, Weiping Yu, Linda A. deGraffenried, Bob G. Sanders, and Kimberly Kline. 2011. "Targeting Cholesterol-Rich Microdomains to Circumvent Tamoxifen-Resistant Breast Cancer." *Breast Cancer Research: BCR* 13 (6): R120. https://doi.org/10.1186/bcr3063.

Toy, Weiyi, Yang Shen, Helen Won, Bradley Green, Rita A. Sakr, Marie Will, Zhiqiang Li, et al. 2013. "ESR1 Ligand-Binding Domain Mutations in Hormone-Resistant Breast Cancer." *Nature Genetics* 45 (12): 1439–45. https://doi.org/10.1038/ng.2822.

Yadav, Bhagwan, Tea Pemovska, Agnieszka Szwajda, Evgeny Kulesskiy, Mika Kontro, Riikka Karjalainen, Muntasir Mamun Majumder, et al. 2014. "Quantitative Scoring of Differential Drug Sensitivity for Individually Optimized Anticancer Therapies." *Scientific Reports* 4 (June): 5193. https://doi.org/10.1038/srep05193.

Zaidi, Nousheen, Leslie Lupien, Nancy B. Kuemmerle, William B. Kinlaw, Johannes V. Swinnen, and Karine Smans. 2013. "Lipogenesis and Lipolysis: The Pathways Exploited by the Cancer Cells to Acquire Fatty Acids." *Progress in Lipid Research* 52 (4): 585–89. https://doi.org/10.1016/j.plipres.2013.08.005.

Zhao, Fei, Ping Xie, Jiali Jiang, Lingqiang Zhang, Wei An, and Yutao Zhan. 2014. "The Effect and Mechanism of Tamoxifen-Induced Hepatocyte Steatosis in Vitro." *International Journal of Molecular Sciences* 15 (3): 4019–30. https://doi.org/10.3390/ijms15034019.

Figures and tables

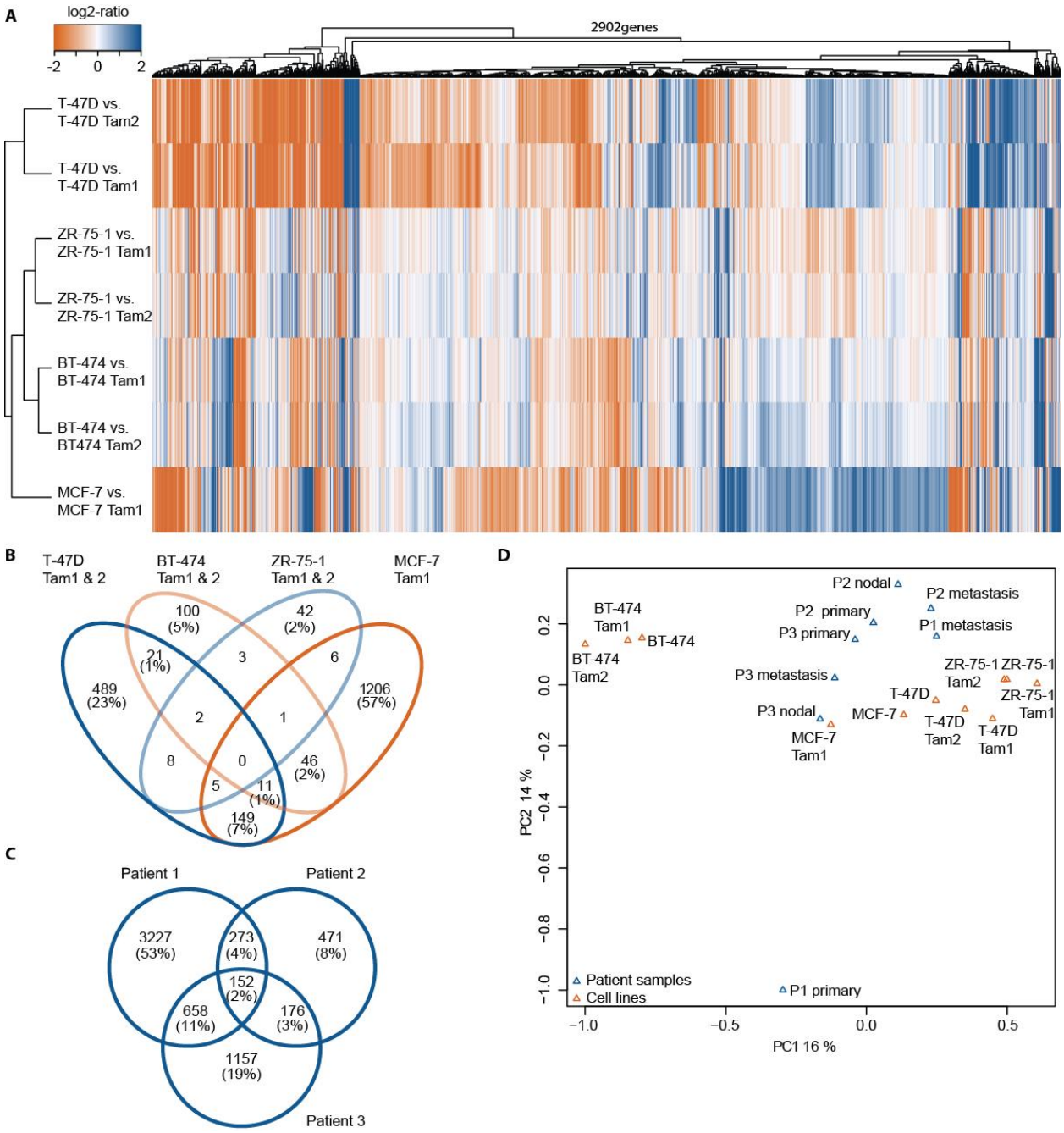

Figure 1: Tamoxifen-resistant cell lines display distinct expression changes and share similarities with patient cases. A Hierarchical clustering and heat map visualization of each parental/resistant cell line pair. Orange (negative log2-ratio) represents increase and blue (positive log2-ratio) decrease in expression in the resistant cell lines. Only protein coding genes with log2 ratio >|1| and the difference of gene expression > |10| CPM in at least one of the comparisons are displayed. Log2 ratios of >= |2| are displayed in the same color. Tamoxifen-resistant clones (B) and patient samples (C) differ in their expression changes. Parental is compared with resistant cell line and primary tumor with metastatic tumor from the same patient, respectively. Venn diagrams show overlap in numbers and percentage of genes that are differentially expressed. D PCA plot indicates that patients share expression patterns with the luminal A cells.

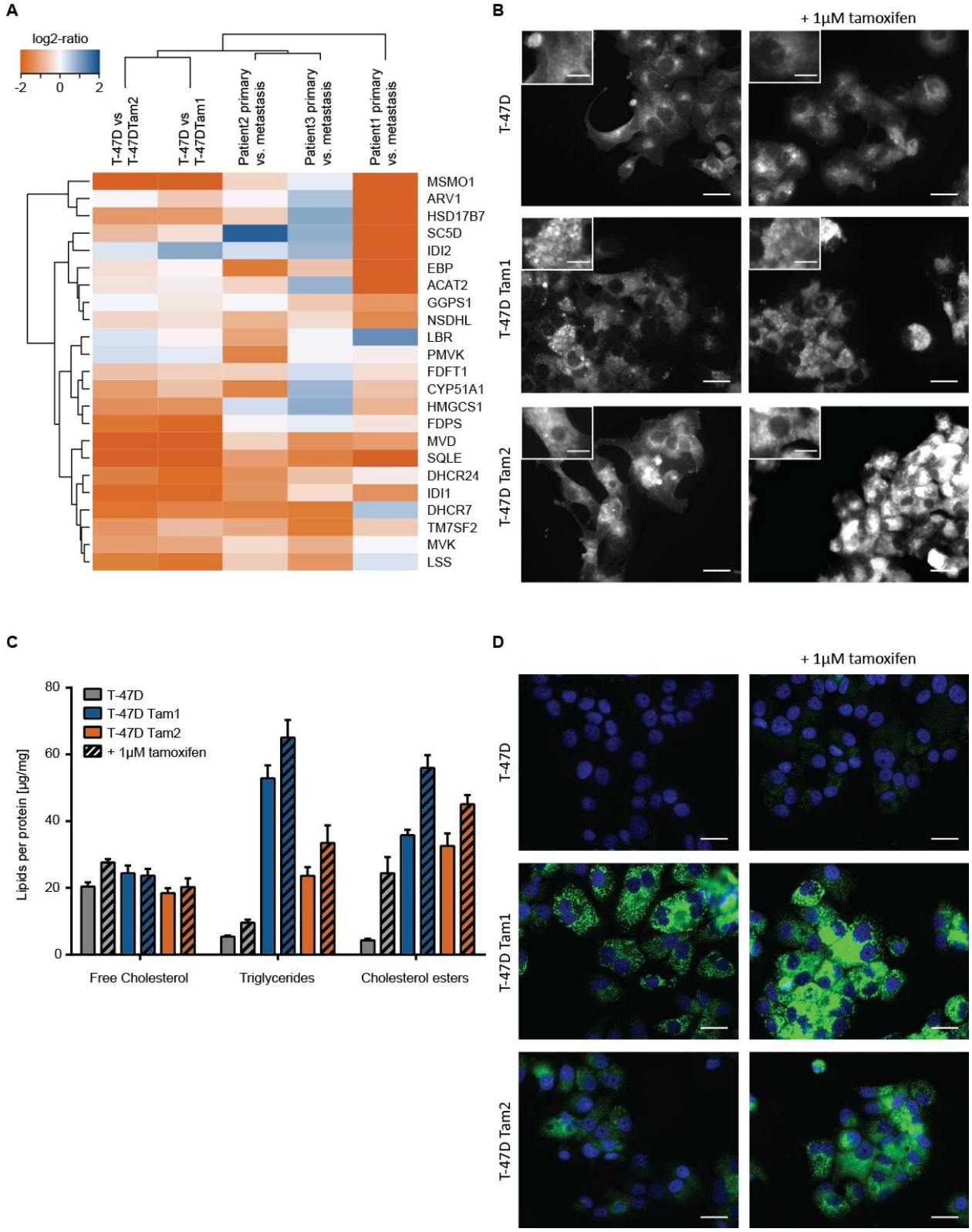

Figure 2: Genes of cholesterol pathway and related lipids are upregulated in the tamoxifen-resistant T-47D cell lines. A Hierarchical clustering and heat map visualization of each parental/resistant cell line pair and patient primary/metastatic tumor. Orange (negative log2-ratio) represents increase and blue

(positive log2-ratio) decrease in expression in the resistant cell lines/metastatic tumor. Log2 ratios of >= |2| are displayed in the same color. B Filipin staining reveals an increase in intracellular amounts of free cholesterol in tamoxifen-resistant T-47D cells +/- 1µM 4-OH- tamoxifen. C Quantification of lipid content in cells grown +/- 1µM 4-OH-tamoxifen reveals an increase in cholesterol esters and triglycerides in tamoxifen-resistant cells (depicted as colored bars). D LipidToxGreen staining of neutral lipids (green) demonstrates that accumulation of neutral lipids into lipid droplets in tamoxifen-resistant cells. The nuclei (blue) were stained with Hoechst.

700

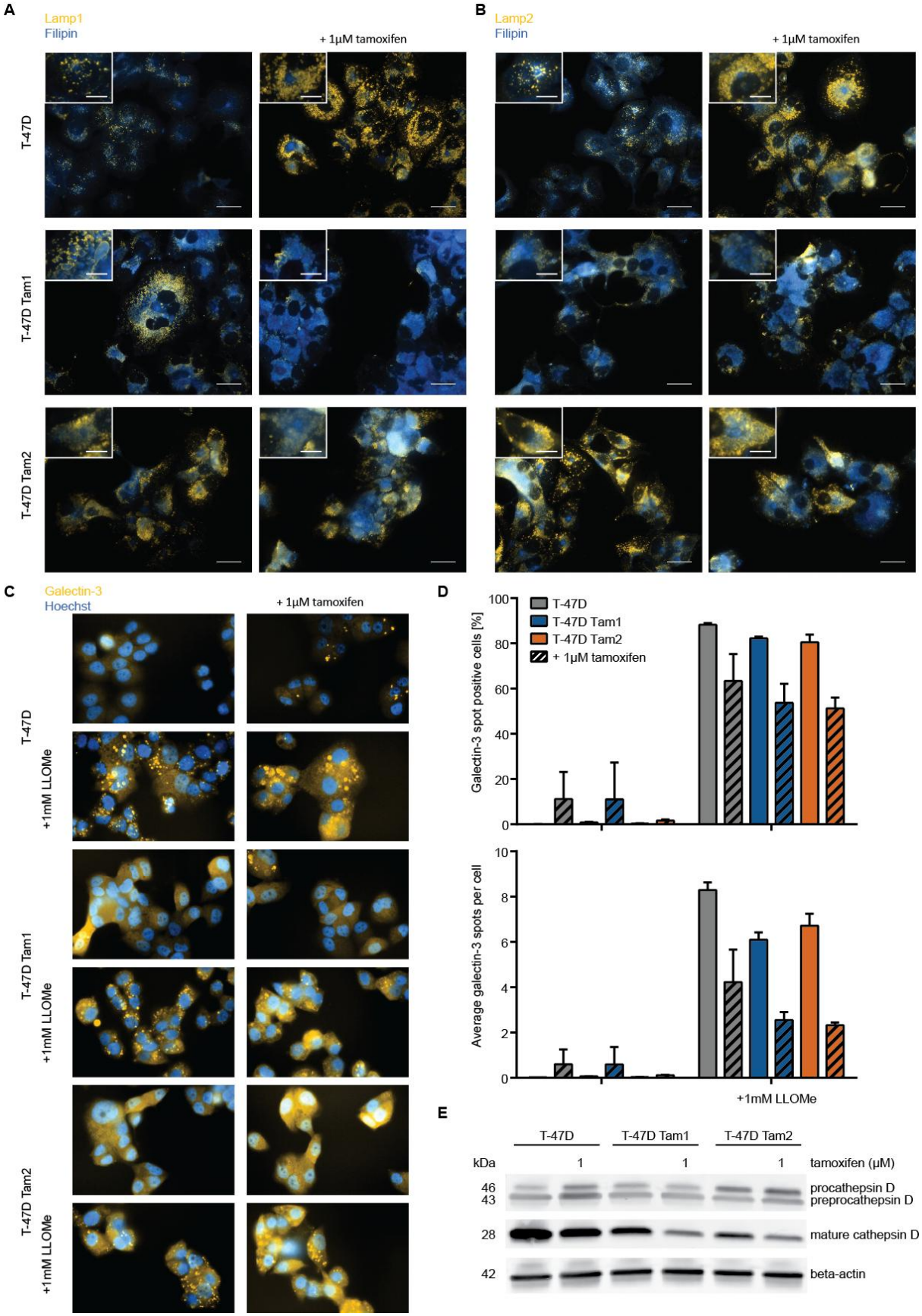
A
Lamp1
Filipin
+ 1µM tamoxifen
T-47D
T-47D Tam1
T-47D Tam2
B
Lamp2
Filipin
+ 1µM tamoxifen
C
Galectin-3
Hoechst
+ 1µM tamoxifen
T-47D
+1mM LLOMe
T-47D Tam1
+1mM LLOMe
T-47D Tam2
+1mM LLOMe
D
T-47D
T-47D Tam1
T-47D Tam2
+ 1µM tamoxifen
Galectin-3 spot positive cells [%]
Average galectin-3 spots per cell
+1mM LLOMe
E
T-47D
T-47D Tam1
T-47D Tam2
kDa
1
1
1
tamoxifen (µM)
46
43
procathepsin D
preprocathepsin D
28
mature cathepsin D
42
beta-actin

Figure 3: Free cholesterol accumulates in lysosomes in the resistant cells. Intracellular accumulation of free cholesterol (blue) accumulates in lysosomes (orange) stained with two lysosomal markers, Lamp1 (A) and Lamp2 (B), detecting the lysosomal-associated-membrane-proteins 1 and 2 +/- 1µM 4-OH-tamoxifen. Tamoxifen-resistant cells are less sensitive to lysosomal membrane premeabilization detected with galectin-3 (orange) translocation (C, images were differently enhanced for visualization purposes) and measurement of galectin-3 positive cells (D upper graph) as well as number of galectin-spots per cell (D

lower image). Galectin-3 measurements were done on the raw image. E Mature cathepsin D is downregulated in tamoxifen resistant cells.

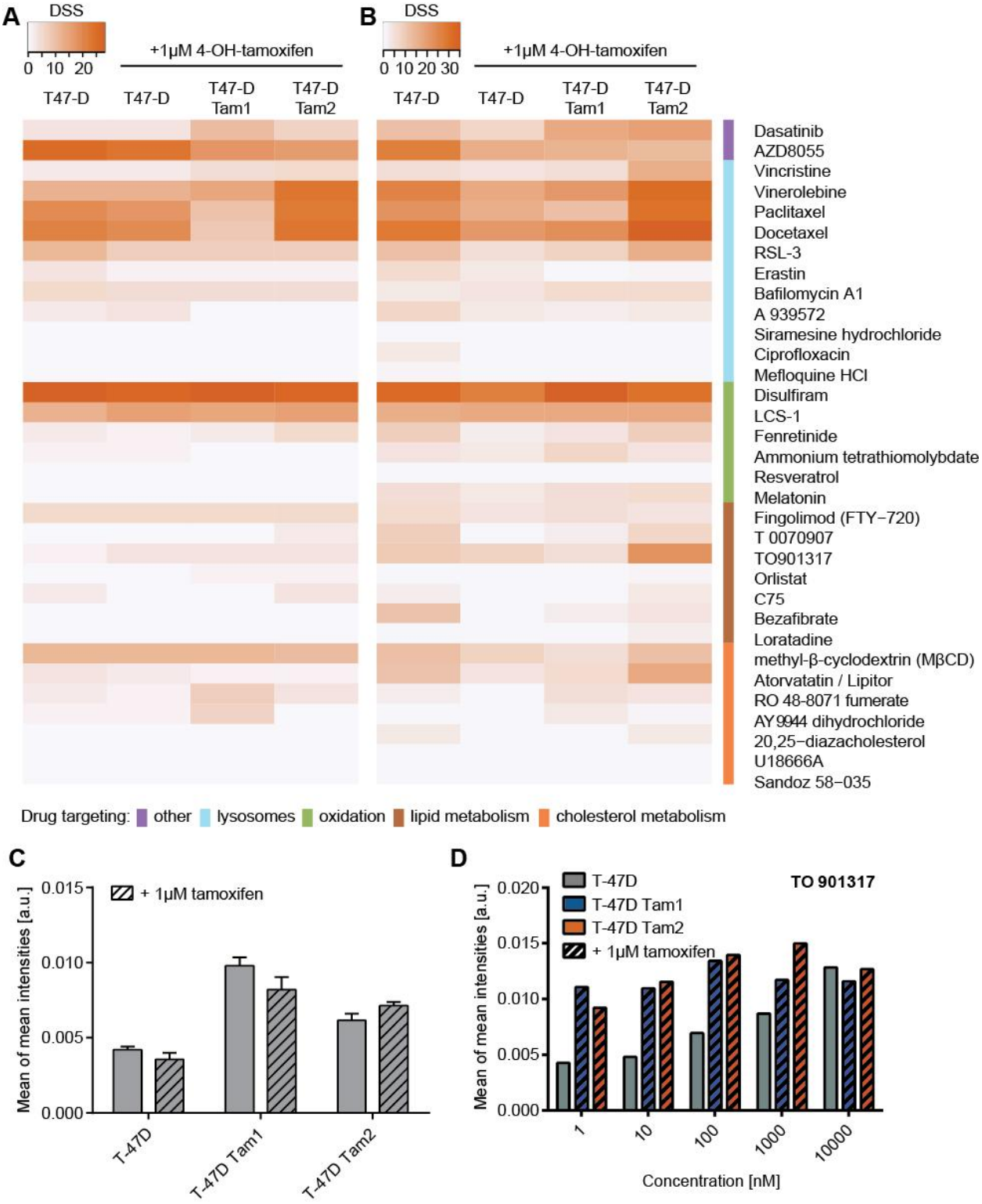

Figure 4: Drug sensitivity and resistance testing of tamoxifen resistant cells. DSS scores of A CTG-measurement and B cell count are displayed as heatmap with dark orange showing the most effective

711 drugs. C Quantification of LipidToxGreen staining in cells grown +/- 1µM 4-OH-tamoxifen reveals an
712 increase in the mean intensities of the staining in tamoxifen resistant cell lines. D TO901317 increases the
713 LipidToxGreen staining mainly in the parental cell lines

714 Table1: Differentially expressed genes

Number of	T-47D Tam1	T-47D Tam2	BT-474 Tam1	BT-474 Tam2	MCF-7 Tam1	ZR-75-1 Tam1	ZR-75-1 Tam2
differentially expressed genes	1425	1239	303	360	1424	193	158
upregulated genes	941	823	195	183	640	104	68
downregulated genes	484	416	108	177	784	89	90

715

716 Table2: TOP5 of gene enrichment in tamoxifen-resistant breast cancer cells using the Reactome 2016
717 pathway analysis. Resistant cell lines are compared with the isogenic parental control cells.

Cell line	Term	Adjusted p-value	Overlap
T47D Tam1	Cholesterol biosynthesis	1,49E-04	11/23
	Platelet activation, signaling and aggregation	1,49E-04	41/253
	Platelet degranulation	1,49E-04	24/105
	Activation of gene expression by SREBF (SREBP)	1,49E-04	14/42
	Response to elevated platelet cytosolic Ca2+	1,49E-04	24/110
T-47D Tam2	Cholesterol biosynthesis	1,28E-07	13/23
	Metabolism of lipids and lipoproteins	1,27E-05	78/659
	Activation of gene expression by SREBF (SREBP)	4,21E-05	14/42
	Platelet activation, signaling and aggregation	2,06E-04	37/253
	Regulation of cholesterol biosynthesis by SREBP (SREBF)	2,06E-05	15/55
MCF-7 Tam1	Cell Cycle	8,40E-13	96/566
	M Phase	1,80E-12	59/268
	Mitotic Cell Cycle	2,93E-12	82/462
	RHO GTPase Effectors	7,30E-11	54/255
	Signaling by Rho GTPases	1,27E-09	65/367
ZR-75-1 Tam1	MHC class II antigen presentation	3,45E-04	9/103
	Mitotic Cell Cycle	6,60E-04	17/462
	Resolution of Sister Chromatid Cohesion	8,75E-04	8/99
	Signaling by Rho GTPases	1,16E-03	14/367
	Mitotic Prometaphase	1,16E-03	8/107
ZR-75-1 Tam2	Extracellular matrix organization	0,0289	10/283
	Platelet degranulation	0,0289	6/105
	Response to elevated platelet cytosolic Ca2+	0,0289	6/110
	PTK6 promotes HIF1A stabilization	0,1142	2/7

	Integrin cell surface interactions	0,1172	4/67
BT-474 Tam1	Axon guidance	7,60E-04	23/515
	Non-integrin membrane-ECM interactions	7,60E-04	7/42
	Developmental Biology	1,15E-03	29/786
	Extracellular matrix organization	2,93E-03	15/283
	Interferon gamma signaling	7,27E-03	8/93
BT-474 Tam2	Diseases of glycosylation	3,54E-06	13/88
	Diseases associated with O-glycosylation of proteins	3,68E-04	11/62
	O-linked glycosylation	1,83E-05	13/110
	Defective GALNT12 causes colorectal cancer 1 (CRCS1)	5,07E-05	6/18
	Defective GALNT3 causes familial hyperphosphatemic tumoral calcinosis (HFTC)	5,07E-05	6/18

Additional figure 1 Tamoxifen-resistant cell lines display distinct expression changes. Tamoxifen-resistant clones derived from same parental cells (A) and of the luminal A subtype (B) differ in their expression changes. Venn diagrams show overlap in numbers and percentage of genes that are differentially expressed.

Additional file 1: Antibodies used in this study
Additional file 2: Drugs used in this study
Additional file 3: RNA-sequencing statistics
Additional file 4: Detected fusion genes of parental and tamoxifen-resistant cell lines
Additional file 5: Batch corrected CPM counts of cell lines and patients
Additional file 6: DSS scores of CTG measurement and cell count
Additional file 7: Mean of the mean LipidToxGreen intensity values